Textures and Microstructures, 1989, Vol. 11, pp. 203–217
Reprints available directly from the publisher.
Photocopying permitted by license only

INFLUENCE OF GRAIN BOUNDARY CHARACTERISTICS AND OF CHEMICAL PARAMETERS ON ABNORMAL GRAIN GROWTH IN Fe–3% Si SHEETS

N. ROUAG and R. PENELLE

Laboratoire de Métallurgie Structurale, UA CNRS 1107, Université Paris Sud, 91405 Orsay Cedex, France

The purpose of the present study was to precise mechanisms at the origin of the exaggerated Goss grain growth of Fe–3% Si sheets, grade Hi–B. It has been pointed out that at the primary recrystallized state, the Goss grains which belong to the small grain class are present through the whole sheet thickness. In presence of AlN and MnS inhibitors, their growth during the anisothermal secondary recrystallization annealing is due to the high mobility of the special C.S.L. boundaries; their subsequent expanse at the fifth of the sheet thickness is favoured by purification of the sheet. Indeed, after dissociation of AlN and MnS precipitates at high temperature, a concentration gradient in sulfur and in nitrogen due to the reducing hydrogen atmosphere has been observed in subsurface thanks to SIMS experiments, such as general and C.S.L. boundaries can easily move whereas those at the center of the sheet are more dragged.

KEY WORDS Grain growth, goss texture, coincidence boundaries, growth inhibition, Fe–S, AlMn, MnS.

1. INTRODUCTION

Industrial making of Fe–3% Si is essentially based on development of a sharp texture $\{110\}\langle 001\rangle$ by secondary recrystallization. The process, due to Goss, has been improved during these last decades, notably by the Nippon Steel Corporation; after hot rolling it is based on combination of cold rolling and thermal treatments under appropriate atmosphere. The $\{110\}\langle 001\rangle$ texture is achieved by abnormal growth of a minority of grains having the Goss orientation; this mechanism, so called exaggerated, or discontinuous growth, is able to start only if normal growth is inhibited. In the case of high permeability material, Hi–B, inhibition of the matrix is due to presence of AlN and MnS precipitates. The use of aluminium nitrides reinforces the sharpness of the secondary recrystallization texture, indeed texture spread decreases from about ten degrees in the case of C.G.O. (Conventional Grains Oriented) to 3–5° for Hi–B sheets.

If, from the industrial point of view, the making process seems to be operational for production of high quality sheets; however fundamental mechanisms which govern Goss texture formation are not still well defined. The onset of the abnormal growth as well as parameters which control it, remain badly known, so that, at the present time, all these questions still stimulate interest of a great number of researchers.

Several studies have been performed from single crystal behavior; evolution of orientations in a single crystal can be a first step to the understanding of the behavior of a textured sheet during recrystallization. So, (110)[001] Fe–3% Si single crystals present the orientation $(\bar{1}11)[211]$ after cold rolling, transformation obtained by a rotation of 35° about an axis $\langle 110\rangle$; after annealing the sample finds again the (110)[001] texture.[1] The same result has also been observed with iron single crystals having the $(\bar{1}11)[211]$ orientation before cold rolling[2] as well as for initially polycrystalline sample. In peculiar, it has been observed that in presence of several components such as $\{111\}\langle uvw\rangle$ after cold rolling, a $\{110\}\langle 001\rangle$ component appears after recrystallization. The main point is that it expands by consuming in a non random way, grains of the primary matrix; the $\{111\}\langle 112\rangle$ component decreases, then disappears more rapidly than the others. These different observations have allowed, since the sixties, to put forward the assumption that the nature of the interface between a crystal having the $\{110\}\langle 001\rangle$ orientation and a crystal $\{111\}\langle 11\bar{2}\rangle$ can play a determinant role for the onset of the growth. Impossibility to characterize the intergranular structure by techniques at that time probably explains the regrettable renounce of this approach to understand the Goss texture formation for more than ten years; so the first studies on industrial materials have essentially considered macroscopic effects, obviously important but not sufficient.

The assumption generally accepted from these studies, is the presence of $\{110\}\langle 001\rangle$ large grains in the matrix after primary recrystallization. These large grains often observed at the fifth of the thickness[3,5] have the advantage of size which allows them to grow in an exaggerated way if the primary matrix is inhibited.

Some authors have suggested a coalescence step from colonies of grains $\{110\}\langle 001\rangle$ observed at the fifth of the thickness.[4]

Development of high permeability sheets (Hi–B) removes the previous assumptions, available in the case of C.G.O. material. Recent studies[3] point out that, if the Goss grains which invade the final matrix are effectively located at the fifth of the thickness, *they do not benefit of a size larger than the average of the grains of the primary matrix.* They are not gathered as colonies and do not represent a texture component which can be detected by X-ray diffraction. Therefore, *the size factor is not a necessary condition to the onset of the abnormal growth.* The Goss grain growth can probably be explained by a particular character of grain boundaries which surround them, as well as from the structural point of view that from the interaction point of view with precipitates. Indeed, the different parameters capable of occuring are not independant: the crystallographic texture, the grain boundaries structure and the role of chemical impurities are tightly linked. The follow-up of evolution of these different parameters can allow to define the adequate neighbourhood, chemical and crystallographic, such as a $\{110\}\langle 001\rangle$ grain is able to grow in an exaggerated way.

II. MATERIAL AND EXPERIMENTAL TECHNIQUES

The present study has been performed on a Hi–B silicon steel sheet composition of which in weight is given in Table 1. The sheets after primary recrystallization

Table 1 Composition of the as received material.

Element	C	Si	S	P	Mn	Cr	Ni	Mo
% Weight	0.057	3.08	0.021	0.008	0.078	0.059	0.0066	0.009
Element	Ti	Al	B	Cu	Sn	Pb	N	
% weight	0.018	0.03	0.00001	0.11	0.011	0.0025	0.0072	

have a thickness of about 320 μm which is reached thanks to only one cold rolling with a reduction amount of 80%

$$\left(\frac{e_0 - e}{e_0} \times 100\right)$$

where e_0 and e are respectively the initial and final thickness. The secondary recrystallization annealing is carried out under "U" hydrogen (dew point within $-18°C$, $-20°C$) with an heating rate equal to $60°C\,h^{-1}$. Preliminary thermal treatments have allowed to precise the temperature from which secondary recrystallization starts: for the mentioned conditions, abnormal growth of $\{110\}\langle 001\rangle$ grains starts around 960°C. In order to follow evolution of crystallographic and chemical parameters previously mentioned, the samples annealed at the following temperatures have been considered: 900–940–960–975 and 990°C. The follow-up of the chemical parameter has required to consider higher temperatures, let be 1020, 1050, 1100 and finally 1170°C.

The possible presence of a gradient of chemical and physical characteristics through sheet thickness got us to consider samples at different depths through the thickness. In general, the center, the fifth and the sheet surface have been considered.

Determination of the crystallographic texture for the different samples has been determined by X-ray diffraction by using a Lucke–Siemens goniometer. The experimental method used in the present study is that in reflection–transmission; the three pole figures {110}, {200} and {211} have been used to calculate the orientation distribution function $F(g)$[6] with an expansion order equal to 22.

Determination of grain boundaries characteristics has been performed by using transmission electron microscopy, KOSSEL patterns and Selected Area Channeling patterns. Evolution of AIN and MnS precipitates has been followed both by thermoelectric power T.E.P. measurements and by Secondary Ion Mass Spectroscopy S.I.M.S.

III. EVOLUTION OF CRYSTALLOGRAPHIC PARAMETERS

At the primary recrystallization state, Figure 1, the as received sheet is characterized by two preferential orientations, Figure 2: a component near $\{111\}\langle 112\rangle$ with $F(g)max \simeq 10$ and a component $\{100\}\langle 012\rangle$ with $F(g)max \simeq 3.5$, their volume fraction is respectively equal 50 and 20%. The Goss orientation, non detected by X-ray diffraction is therefore less than 5%, an estimation from metallographic observations allows to estimate it at about 10^{-2}%.

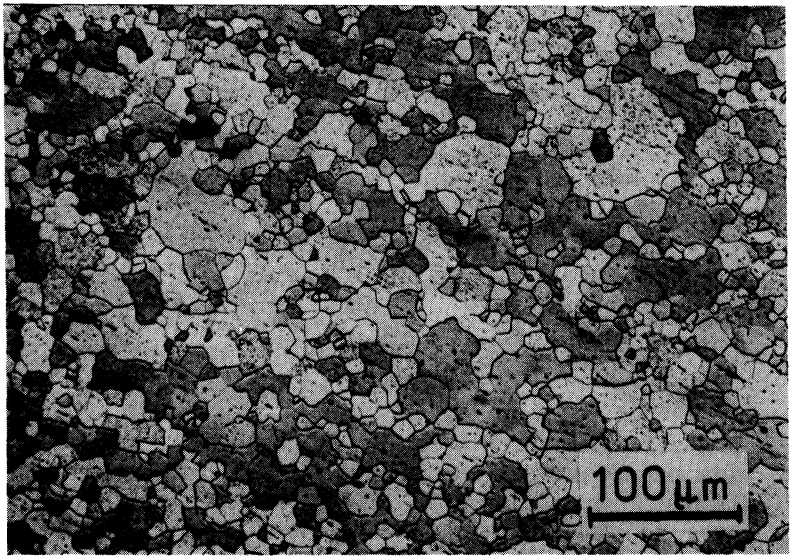

Figure 1 Microstructure after primary recrystallization: as received material.

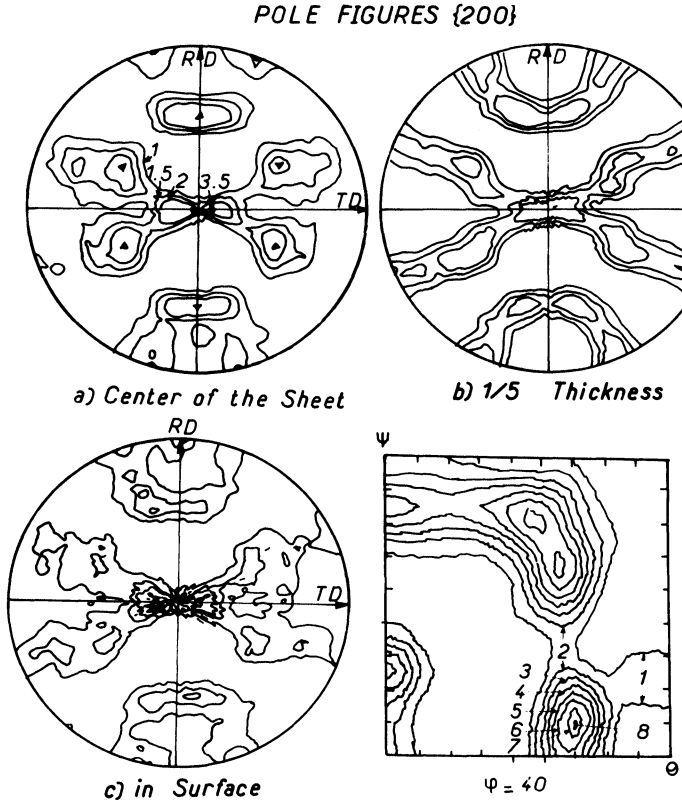

Figure 2 {200} pole figure of the as received material: a) center of the sheet; b) at the fifth of the thickness; c) at the surface. ODF diagram at 1/5 thickness and at $\varphi = 40°$.

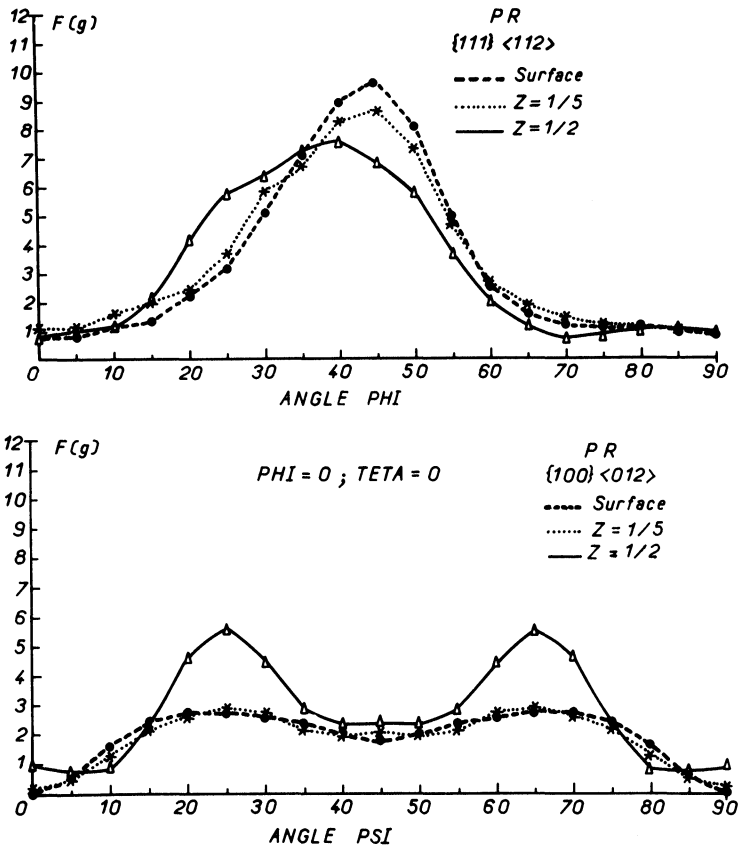

Figure 3 Variation of the ODF along the skeleton line: a) component {111}⟨112⟩; b) component {100}⟨012⟩.

For the two main components, a smooth texture gradient has been detected through the sheet thickness, Figure 2. The components near {111}⟨112⟩ and near {100} ⟨012⟩ respectively decrease from 10 to 8 and from 6 to 3, Figure 3, from the surface to the center of the sheet.

Determination of the nature of grain boundaries has been performed from local texture studies. At this scale no gradient of the crystallographic characteristics has been observed through sheet thickness, Figure 4, indeed there is no perceptible difference between the surface and the center of the sheet, the percentage of C.S.L. (Coincidence Site Lattice) grain boundaries at the primary recrystallized state is about equal to 12–13%. However, it can be remarked that the percentage of C.S.L. grain boundaries is greater than that of an isotropic material for which it is equal to 9–10%. This points out the presence of *a texture in the grain boundaries distribution* because of the crystallographic texture.

During the final recrystallization annealing, it is worth noting that the component having a {100} plane parallel to the sheet plane is quite stable, whereas the component of {111} plane tends to decrease during the normal growth. These two different behaviours are also displayed when the abnormal

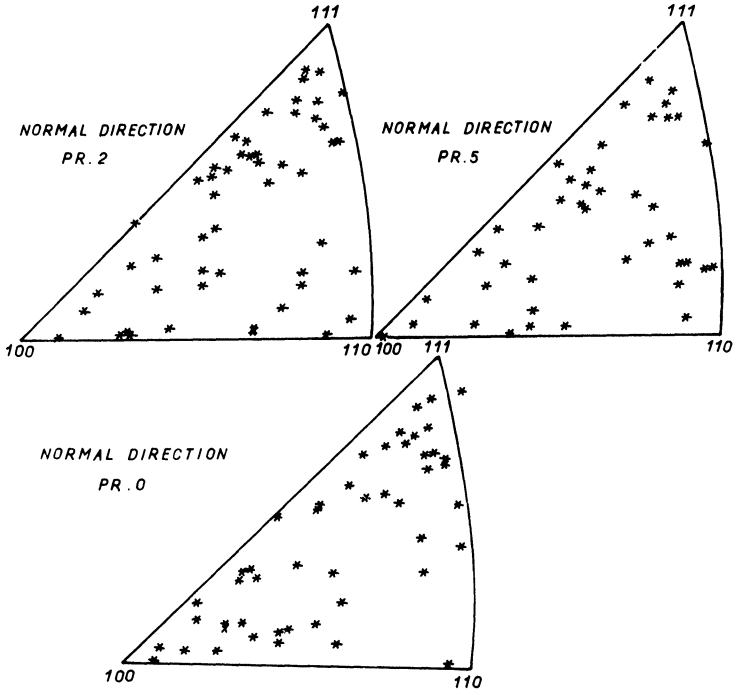

Figure 4 Distribution of crystallographic directions parallel to the normal direction to the sheet plane through the sheet thickness.

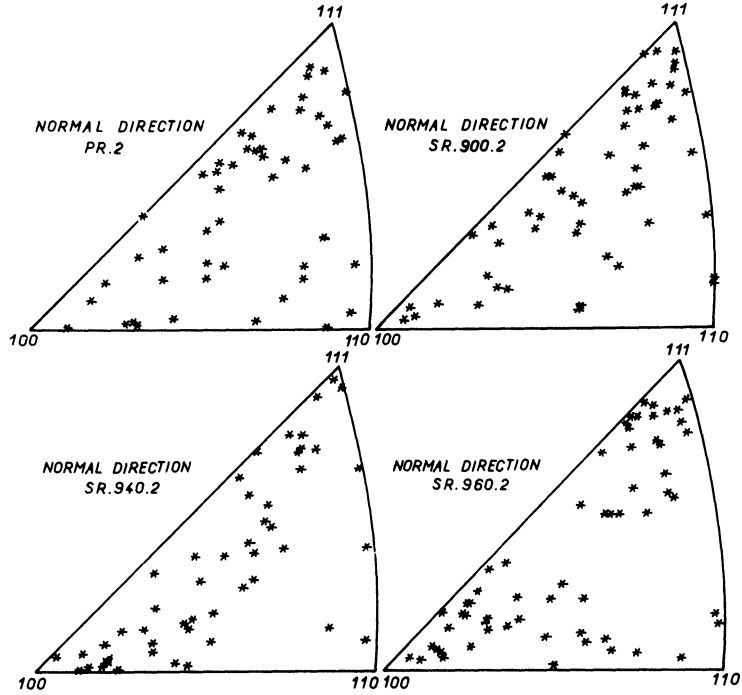

Figure 5 Distribution of the normal directions in a unit triangle at the primary state PR and after secondary recrystallization at different temperatures.

growth begins, as it is shown on, Figure 5. It is also worth noting that the close neighbourhood of the Goss grain is notably perturbed as soon as the abnormal growth starts: the component {111} disappears more rapidly than the {100} one. Therefore it seems that the exaggerated growth of the Goss grain occurs firstly at the expense of the {111} ⟨112⟩. The behaviour of the Goss grain being different relative to the two preferential orientations of the matrix, this observation involves a difference in the mobility between the two types of grain boundaries: Goss component—{111}⟨112⟩ and Goss component—{100}⟨012⟩. At this step, it can be noticed that the misorientation between a {110}⟨001⟩ grain with a {111}⟨112⟩ grain corresponds to a coincidence boundary, let be 4° Σ9, whereas the misorientation between {110}⟨001⟩ and {100}⟨012⟩ corresponds to a general boundary.

Then, it appears that the boundaries of C.S.L. type are more mobile than the general boundaries at the beginning of the abnormal growth.

This assumption is confirmed by evolution of the percentage of C.S.L. boundaries surrounding the growing grain as it can be seen Table 2.

It is worth noting that at 960°C, the percentage of C.S.L. boundaries has been calculated by immersing a Goss grain in the real matrix. For 975 and 990°C, this percentage has been determined experimentally; we can see that the percentage of C.S.L. boundaries decreases notably between 960 and 975°C then increases to reach at 990°C a value equal to that of the mean distribution of the matrix at a step where the abnormal growth is more advanced.

To understand this behaviour, firstly it has to be reminded that the abnormal growth starts whereas the impurities are still in precipitates form. The maximum dragging force F exerted on grain boundaries is then given by:

$$F = K\gamma_b \frac{f}{r} \tag{1}$$

where K is a shape factor, γ_b the grain boundary energy, f the volume fraction of particles and r their radius. This force is proportional to grain boundaries energy; therefore coincidence grain boundaries corresponding to minimums of energy are less dragged by precipitates than the general boundaries. As far as the impurities are in form of precipitates, the formers are relatively more mobile than the latters.

So it can be assumed that the first step of the abnormal growth is controlled by the speciality of grain boundaries: the abnormal growth of a Goss grain can occur more easily because the Goss grain owns more C.S.L. boundaries, these ones[8] being less dragged by precipitates and that because of the presence of the {111}⟨112⟩ component.

Table 2 Evolution of the distribution of C.S.L. grain boundaries around a Goss grain.

Annealing temperature °C	960	975	990
% C.S.L.	13	5	12.5

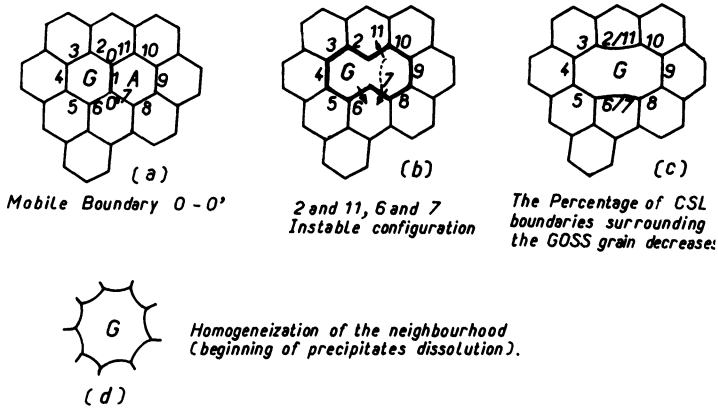

Figure 6 Scheme of the abnormal growth of a Goss grain G at the expense of a {111}⟨112⟩ grain, 0–0′ is a CSL boundary.

Evolution mentioned from the Table 2 is due to different behaviour of boundaries surrounding the growing Goss grain; Figure 6 schematizes this evolution in two dimensions. It has to be recalled that the volume fraction of the Goss grain is very small, 10^{-4}. So the Low Angle, (L.A.) boundaries, very stable, are not to be considered for growth of Goss grain in the first steps of the abnormal growth.

In order that a grain can grow, it has to own a minimum of six sides; if this condition is fulfilled and if we take into account the condition proceeding from the assumption of grain goundary speciality, it owns at least a C.S.L. boundary. At 960°C, temperature for which the abnormal growth starts, the Goss grain is surrounded in average by 13% of C.S.L. boundaries. As it has been observed at least at the beginning of the abnormal growth that the Goss grains belong to the population of small grains, therefore surrounded by a few boundaries, there is a reasonnable probability in order that this condition is verified. So, let us consider the most probable case where the Goss grain has at the beginning a C.S.L. boundary, Figure 6a. Figures 6b and c display the following step: the Goss grain has grown at the expense of a grain belonging to the component {111}⟨112⟩ for instance. The boundary 0–0′ by moving, breaks the equilibrium of the two triple points 0 and 0′; the boundaries 11 and 7 disappear during the displacement of the boundary 1, let be 0–0′. Among all the boundaries which surround the new grain, two groups have to be considered;

—the new boundaries, 8 to 10 on the figure; among these boundaries, there will be, in average always a C.S.L. boundary which will allow it to continue its growth.

—the old boundaries, 2 to 6 on the figure, among which there is no more C.S.L. boundary, consequently the percentage of C.S.L. boundaries will decrease.

On a general way, the probability to meet a C.S.L. boundary remains the same, whereas the total number of boundaries surrounding the grain increases as the Goss grain grows. This involves a decrease of the percentage of C.S.L. boundaries in agreement with experimental observations. The step b and c will

occur as far as the difference in mobility between C.S.L. boundaries and general ones remains.

The step d points out a state more advanced of the abnormal growth. For higher temperatures, the difference of mobility between C.S.L. and general boundaries decreases, so that there is an homogeneization of growth rate; therefore the mean fraction in C.S.L. boundaries of the beginning is found again. So the case d is in agreement with the experimental step 975–990°C.

So it seems that the first step of the Goss texture formation by secondary recrystallization is controlled, in presence of AlN and MnS precipitates, by the crystallographic parameter: a percentage of C.S.L. boundaries greater than the mean value of the matrix is necessary in order that the $\{110\}\langle 001\rangle$ starts its abnormal growth. Existence of the $\{111\}\langle 112\rangle$ in the primary matrix gives the good crystallographic neighbourhood in order that this condition is fulfilled.

The presence of the $\{111\}\langle 112\rangle$ orientation gives in fact to the Goss grains a probability greater than the average in the matrix to have mobile boundaries. However existence of mobile boundaries surrounding this grain will allow either its growth or its shrinkage.

Indeed if we consider that, case a of the Figure 6, the boundary 0–0′ between the Goss grain and a grain $\{111\}\langle 112\rangle$ is a C.S.L. boundary, therefore mobile; then, there are two possibilities to consider: either the boundary 0–0′ moves in the sense of the growth of the Goss grain or on the contrary, in that of its shrinkage, with the same probability.

—If the boundary 0–0′ moves in the sense G→A, then the Goss grain will grow. It always has the same probability to own an other mobile boundary, the choice between growth and shrinkage will remain until the size of the Goss grain is clearly larger than the average of the matrix. The size factor becomes important and the Goss grain will continue its growth.

—If the boundary 0–0′ moves in the sense A→G, the Goss grain will shrink in favour of the grain A. On the other hand, contrary to the previous case, the probability in order that the grain A owns an other boundary of the same type C.S.L. is practically equal to zero, because of the very small volume fraction of Goss grains in the matrix.

Obviously it has to be taken into account that the other grains of the matrix can also form special boundaries between them. In the same way that for the Goss grain, the hypothetic boundaries formed between the grains $\{111\}\langle 112\rangle$ and $\langle 100\}\langle 012\rangle$ and those of the rest of the matrix at 960°C have to be considered. Table 3 gathers these estimations with that of the Goss grain.

So the probability to have C.S.L. boundaries for the matrix components is less than that of the Goss grain. Moreover, the probability to have stable Low Angle boundaries has to be taken into account in the case of these two orientations, which correspond to the main components of the tacture of the sheet, contrary to

Table 3 Fraction of C.S.L. boundaries formed by the three orientations, Goss, *A* and *B* with the matrix at 960°C at the fifth of the thickness.

Orientation	$G = \{110\}\langle 001\rangle$	$A = \{111\}\langle 112\rangle$	$B = \{100\}\langle 012\rangle$
% C.S.L.	13	10	8

the Goss grain for which this probability is practically equal to zero, except at the final state of the secondary recrystallization annealing.

The primary matrix, characterized by the two components $\{111\}\langle 112\rangle$ and $\{100\}\langle 012\rangle$ allows the Goss grain to have "the good crystallographic neighbourhood" to begin its abnormal growth.

Let us remind that at the beginning the Goss grain does not benefit of the size advantage to grow in an exaggerated way. In fact the onset of the abnormal growth which is controlled by the speciality of the boundary is not in contradiction with the Hillert's theory:[9] the nature of the grain boundary allows the Goss grain to get this advantage of size which controls in part the final steps of the abnormal growth.

IV. BEHAVIOUR OF THE INHIBITORS

The role of precipitates in the formation of the Goss texture shows a preferential behaviour of grain boundaries according to minimums of energy, get more rapidly the driving force necessary to overcome the dragging force. In other respects, this force being inversely proportionnal to the size of precipitates, inhibition of the primary matrix by AlN precipitates is more efficient than that obtained by managanese sulfides. Table 4 shows the ratios of the relative dragging forces for the two types of precipitates, distribution of which is displayed Figure 7. So it can be noted that efficiency concerning the matrix inhibition is in a ratio 3 between the two types of precipitates. This ratio remains practically constant during the normal growth.

These observations confirm the prevaling action of the aluminum nitrides as inhibitors. In others respects it has been observed that precipitation of AlN is not complete after primary recrystallization, indeed precipitation continues at the beginning of the secondary recrystallization annealing. Image analysis of precipitates has shown that the volume fraction of AlN increases of about 10%; this result is confirmed by the variation of the thermoelectrical power which increases slightly what corresponds to a decrease of the solute concentration in the matrix.

Inhibition of the matrix by impurities such as precipitates constitutes a first aspect of the role of the chemical parameter for the formation of the Goss texture by secondary recrystallization. An other aspect concerns the purification of the material after dissolution of the precipitates.

Table 4 Evolution of the relative efficiency of the two types of precipitates AlN and MnS.

	Primary recrystallization	900°C	960°C
$\frac{\sum_i^{N_{AlN}} f_i/r_i}{\sum_i f_i}$ (AlN)	0.014 $N_{AlN} = 10$	0.013 $N_{AlN} = 10$	0.012 $N_{AlN} = 10$
$\frac{\sum_i^{N_{AlN}} f_i/r_i}{\sum_i f_i}$ (MnS)	0.004 $N_{MnS} = 40$	0.004 $N_{MnS} = 39$	0.004 $N_{MnS} = 37$
$\frac{\text{Dragging AlN}}{\text{Dragging MnS}}$	3.5	3.2	3.0

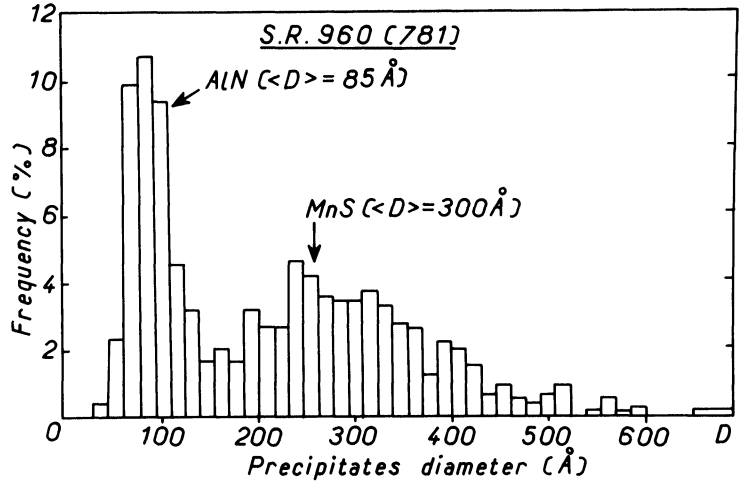

Figure 7 Distribution in size of AlN and MnS inhibitors just at the onset of the abnormal growth.

From the variation of the thermo-electrical power, Figure 8, which is as it has been underlined sensitive to the concentration in solute elements (when the concentration in sulfur increases, the T.E.P. decreases and conversely), it can be noted two temperatures of dissolution: the first around 990°C, corresponding probably to the complete dissolution of aluminium nitrides and the second around 1050°C to manganese sulfides.

By an other way, the split from 990°C between the two curves, corresponding from one hand to the whole thickness of the sheet and from an other to the sample for which one fifth of the thickness has been removed from the surface, points out the presence of a gradient of concentration which takes place during the last steps of the secondary recrystallization annealing. This fact has been

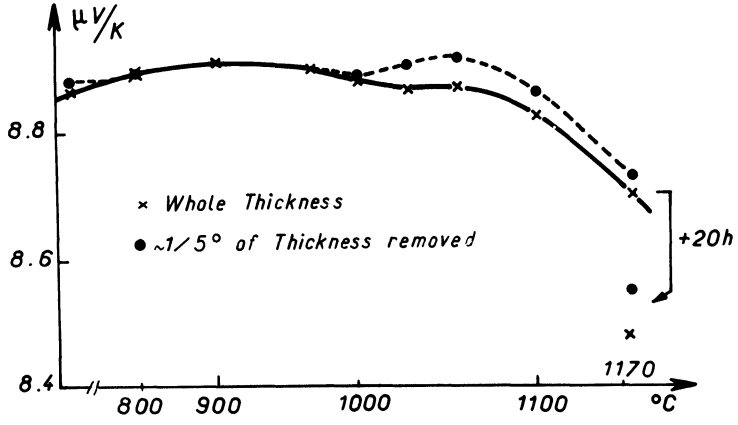

Figure 8 Variation of the thermo-electrical power T.E.P. as a function of annealing temperature.

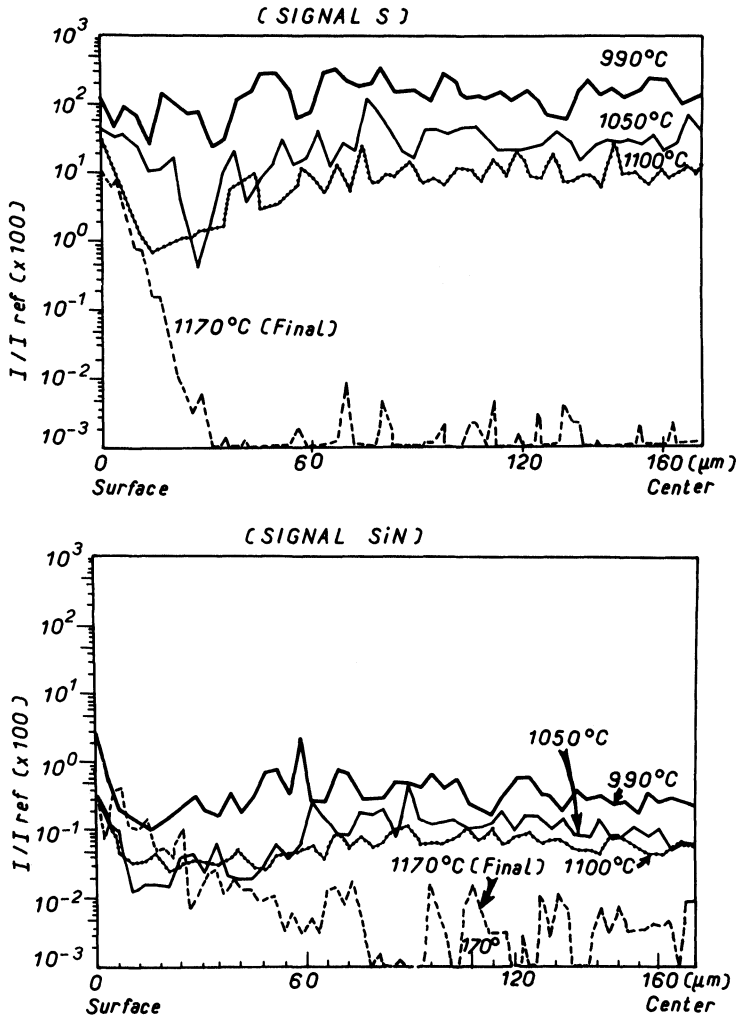

Figure 9 Secondary Ion Mass Spectroscopy results: a) variation of the signal S as a function of the sheet thickness; b) variation of the signal SiN as a function of the sheet thickness.

confirmed by Secondary Ion Mass Spectroscopy (S.I.M.S.) by bombarding an oblique section of a sample with Cs^+ ions.

Figures 9a and b show that a sulfur and nitrogen concentration gradient through sheet thickness takes place after dissolution of AlN and MnS. It can be observed a decrease of the solute concentration in subsurface, decrease which becomes more pronounced when the temperature increases. This difference of concentration can provide an element concerning the comprehension of Goss grain growth. Indeed, the purification of the matrix in subsurface allows the Goss grains located at this depth to continue more easily their growth relative to those nearer the center of the sheet where the abnormal growth starts too but where the concentration in solute elements remains higher.

It is important at this level to underline the importance of the nature of the atmosphere, indeed the concentration gradient in sulfur and in nitrogen occurs thanks to the chemical potential gradient due to the reducing character of hydrogen.

V. CONCLUSION

Different observations performed for this study allow to put forward the assumption that the onset of the abnormal growth is essentially controlled by an aspect crystallographic. The problem of the abnormal growth of the Goss grains is linked to the presence of an adequate neighbourhood thanks to the $\{111\}\langle 112\rangle$ component which ensures to the Goss grains to have a probability relatively high of C.S.L. boundaries, that means mobile boundaries in presence of precipitates. This behaviour of the $\{110\}\langle 001\rangle$ grain appears to be in agreement with the growth grain model proposed by Abbruzzese and Lucke[10–11] indeed:

—The Goss grains which grow, belong to the class of small grains of the matrix whatever the orientation of the other grains. Their size is about equal to 10 μm whereas that of the other grains of the matrix spreads to 60 μm.

—The small volume fraction φ^G of the Goss grain is roughly equal to 10^{-4}, that φ^A of the component $\{111\}\langle 112\rangle$ is equal to 50%, that φ^B of the component $\{100\}\langle 012\rangle$ to 20% and that φ^{iso} of the random to 30%.

—The mobility of a boundary between a Goss grain and a grain having the orientation $\{111\}\langle 112\rangle$ is higher than the mean mobility of boundaries between the other grains due to the fact that it is C.S.L. at the onset of the secondary recrystallization.

Let us remind that the model of Abbruzzese and Lucke considers two orientation classes whose one is larger than the other; three cases can be considered:

—case a: the minority G belongs to the large grains of matrix,

—the two components have the same mean size,

—the minority G belongs to the small grain size class of the matrix.

The high mobility of the C.S.L. boundaries relative to general boundaries because of the presence of AlN and MnS precipitates allows, in the expression of the diffusivity $\tilde{M}^A$ for a class of texture A with a critical radius $\tilde{R}_C^A$ defined by:

$$\tilde{M}^A = \frac{\sum_G M^{AG} \varphi^G \bar{R}^{2G}}{\bar{R}^2} \tag{2}$$

$$\tilde{R}_C^A = \frac{\sum_G M^{AG} \varphi^G \bar{R}^{2G}}{\sum_G M^{AG} \varphi^G R^2} \tag{3}$$

where

M^{AG} = diffusivity between two orientation classes A and G

φ^G = volume fraction of grains having the orientation G

$\bar{R}^G$ = mean radius of the class G

$\bar{R}$ = mean radius of the matrix grains

only to keep the term M^{AG} corresponding to the diffusivity of the special boundary between the grain A and the grain with the orientation G, indeed $M^{AG} = M^{GA} \gg M^{AA} = M^{GG}$ what gives:

$$\tilde{M}^A = \frac{\varphi^G M^{AG} \bar{R}^{2G}}{\varphi^A \bar{R}^{2A} + \varphi^G \bar{R}^{2G}} \tag{4}$$

and

$$\tilde{M}^G = \frac{\varphi^A M^{AG} \bar{R}^{2A}}{\varphi^A \bar{R}^{2A} + \varphi^G \bar{R}^{2G}} \tag{5}$$

$$\tilde{R}_C^A = \frac{\bar{R}^{2G}}{\bar{R}^G} = R_C^G \quad \text{and} \quad \tilde{R}_C^G = \frac{\bar{R}^{2A}}{\bar{R}^A} = R_C^A \tag{6}$$

R_C^A and R_C^G are partial critical radii for the partial distributions φ_i^A, φ_i^G consisting only of A or of G grains. In the present study we have $\varphi^G \ll \varphi^A$ so that $\tilde{M}^G \gg \tilde{M}^A$, as moreover $\bar{R}^G < \bar{R}^A$ only very few Goss grains can grow to a large size. Our results which take into account the speciality of the grain boundary and its mobility because of the good neighbourhood $\{111\}\langle 112\rangle$ around the Goss grain are in agreement with the model proposed by Abbruzzese and Lucke.

In addition to the crystallographic factor of the boundary, the role of the purification of the material during the final annealing has to be taken into account after dissociation of the precipitates.

The Goss grains which are present through the whole sheet thickness begin their growth everywhere, however their abnormal growth in subsurface is facilitated from one hand by the fact that the main component $\{111\}\langle 112\rangle$ is sharper near the surface and from an other hand that the second texture component $\{100\}\langle 012\rangle$, less favourable to the Goss grain growth, is smoother near the surface. Moreover during the secondary recrystallization annealing firstly a dissociation of the AlN and MnS precipitates, is observed, then a purification of the matrix by diffusion of sulfur and of nitrogen to the surface thanks to presence of a gradient of chemical potential due towards the reducing hydrogen atmosphere. If the final annealing is performed under an Argon atmosphere an abnormal growth of Goss grains is still observed because of the good crystallographic parameters, however the proportion of the primary matrix, non consumed remains very important in absence of purification.

ACKNOWLEDGEMENTS

The authors would like to thank Usinor Isbergues for providing Fe–3% Si sheets, IRSID for SACP determination facilities, Dr. M. Aucouturier for SIMS experiments, Dr Borelly for T.E.P. determinations and Dr Hsun Hu for very fruitful discussions.

References

1. Hu, H. *Recovery and Recrystallization of Metals*, L. Himmer Ed., Interscience Publishers, N.Y., 1963, p. 311.
2. Penelle, R. and Lacombe, P. *Textures in Research and Practice*, J. Grewen and G. Wassermann, Eds. Springer-Verlag, Berlin, 1969, p. 267.

3. Rouag, N., Vigna, G. and Penelle, R. 7th Int. Symp. on Metallurgy and Materials Science, N. Hansen, J. Jensen, T. Leffers, B. Ralph, Eds., Riso Denmark, 1986, p. 521.
4. M. Matsuo, T. Sakai, M. Tanino, T. Shindo and S. Hayami, Proceeding of the 6th Int. Conf. on Textures of Materials, I.S.I.J., Ed., Tokyo, 1982, p. 918.
5. Harase, J., Shimisu, R. and Watanabe, T. 7th Int. symp. on Metallurgy and Materials Science, N. Hansen, J. Jensen, T. Leffers, B. Ralph, Eds., Riso Denmark, 1986, p. 343.
6. Masson, C., Parnière, P., Penelle, R. and Pernot, M. (1973). *Mem. Sc. Rev. Met.*, **70,** p. 271.
7. Vigna, G. "Application des techniques de canalisation d'électrons et de Kossel à l'étude de la texture locale et des contraintes internes de tôles de Fe–3% Si". Thèse de Doctorat en Sciences, Université Paris Sud, Orsay, 1987.
8. Aust, K. T. *Textures in Research and Practice,* J. Grewen and G. Wassermann, Eds., Springer-Verlag, Berlin, 1969, p. 160.
9. Hillert, M. (1965). *Acta Met.* **13,** p. 227.
10. Abbruzzese, G. and Lucke, K. (1986). *Acta Met.* **35,** 5, p. 905.
11. Eichelkraut, H., Abbruzzese, G. and Lucke, K. (1988). *Acta Met.*, **36,** 1, p. 55.